FACTA UNIVERSITATIS
Series: **Mechanical Engineering**
https://doi.org/10.22190/FUME230128016A

Original scientific paper

MECHANICAL CHARACTERISTICS OF NANO-CRYSTALLINE MATERIAL IN METALLIC GLASS FORMERS

Hamid Al-Abboodi[1], Huiqing Fan[2], Mohammed Al-Bahrani[3], Abdelsalam Abdelhussien[4], Barhm Mohamad[5]

[1, 2]State Key Laboratory of Solidification Processing, School of Materials Science and Engineering, Northwestern Polytechnical University, Xi'an, China
[1]Kut Technical Institute, Middle Technical University, Wasit, Iraq
[3]Chemical Engineering and Petroleum Industries Department, Al-Mustaqbal University College , Babylon, Iraq
[4]School of Mechanical Engineering, Nanjing University of Science and Technology, Nanjing, China
[5]Department of Petroleum Technology, Koya Technical Institute, Erbil Polytechnic University, Erbil, Iraq

Abstract. *In order to evaluate the model metallic glass alloy's mechanical properties (Fe49.7 Cr17.1 Mn1.9 Mo7.4 W1.6 B15.2 C3.8 Si2.4) prepared by spark plasma sintering (SPS) which have high velocity. We made an apparatus having three-point curve testing. The comparatively bulk sizes of sample in the current study permitted the creation samples for test with a macro scale cross-section (range of mm) consistent test dimensions, and well-controlled sample sizes. Cutting using a wire saw produced remarkably sharp notches with a radius that was 3 times smaller than in earlier studies. Our three-point bending apparatus allowed us to acquire the 231 GPa and 4.91 MPam1/2 values for notch fracture toughness and young's modulus. Additionally, the results of the Vickers indentation and flexure tests for young's modulus were reliable. Vickers indentation measurements of indentation fracture toughness produced values that were a minimum of 49.9% lower than those obtained flexure using. The method for examine micro scale mechanical properties described in this study and the accompanying scrutinizes are valid to samples with different ones or compositions that are made by further means.*

Keywords*: Metallic glass, Three-point bending, Fracture toughness, Vickers indentation, SPS*

Received: January 28, 2023 / Accepted May 07, 2023
Corresponding author: Barhm Mohamad
Department of Petroleum Technology, Koya Technical Institute, Erbil Polytechnic University, 44001 Erbil, Iraq
E-mail: (barhm.mohamad@epu.edu.iq

1. INTRODUCTION

Comparing bulk metallic glasses (BMGs) to crystalline forms of similar compositions, BMGs typically have greater hardness and yield strength values [1, 2]. The metallic glasses are currently being applied include ship manufacturing, boiler fireboxes, the nuclear industry, and the auto industry [3]. However, as their principal weaknesses are frequently low ductility and weak fracture toughness, work is still being done to enhance these qualities [4–9]. This necessitates advancements in material processing as well as the creation of precise methods for calculating fracture toughness. Although there are many ways for measuring the mechanical characteristics of the macroscale sample, it is frequently impractical to employ typical testing methodologies for the marginal's metallic glasses formers because of the processing restrictions on samples size which can be acquired from these types of materials. SPS [10–13] is a pressure-assisted pulsed-current process in which the powder samples are loaded in an electrically conducting die and sintered under a uniaxial pressure and could circumvent the samples size problem for the marginals glass former, enabling the measurement of macroscale characteristics [14–16]. Indentation has been used to quantify the fractures and toughness of the Fe-base metallic glass [17–19], while the notch toughness and test has been done on the sample with the nonstandard shapes [7, 19, 20]. A brittle material's indentation fracture test is unreliable due to the poorly defined cracks in arrested state which makes the analysis more difficult when it is compared with rapid through crack propagations of the standardized test, even though it is most frequently used for samples of small size [21, 22]. As a result, the indentation-based data on mechanical characteristics show significant disparities. Consequently, using a standardized method like three-point bending to determine fracture toughness is more accurate. Testing metallic glasses for three-point bend, however, may yield results that don't seem reliable. For instance, recent three-point bending tests of the fracture toughness of Zr-based metallic glass revealed a significant amount of data scatter [21]. It is acknowledged that thermoplastic forming, such as SPS, provides superior controls over the samples heat history is to minimize the processing's induced dispersion, and that this is type of processing issues rather than testing's issue [22]. Three-point bending has also been used to determine the fractures toughness of the Fe-base metallic glass, however, test of specimen and the notch used had irregular geometries which could lead to inaccuracies. Metallic glasses have undergone fractures toughness test with the notch machined using the electric discharge machine (EDM) [21, 23], the heating brought on by the EDM could cause volumes of the materials in heat affected zones to crystallize or even crack, which may result in inaccurate fractures and toughness value.

In current study, techniques for evaluating Fe based BMGs are developed for increasing precision of the measurements of the fracture's toughness and the modulus of the marginals glass former. The model marginals glass formers, SAM2X5, along with notional compositions of $Fe_{49.7}Cr_{17.1}Mn_{1.9}Mo_{7.4}W_{1.6}B_{15.2}C_{3.8}Si_{2.4}$, was produced in bulk samples using SPS. The production of the test's specimen with the macroscales cross section (in millimetres range) and the well control samples dimension are close to the standardized test. This was made possible in the current investigation due to the comparatively high sample size. The samples' increased sizes also made it possible to examine changes both within and between individual samples. A remarkably sharped notch with radius of (3X smaller than in earlier research) the little samples damage was

possible with a wire saw cutting. These samples were tested for fracture toughness and flexural modulus using a mechanical testing device that was specifically designed for the purpose. There isn't any data on fracture toughness that can be directly compared because the values presented in this paper were determined using a novel approach on a material that underwent SPS processing. As a result, we attempted to compare the numbers obtained from our novel three-point bending technique to those obtained from indentation tests on our material, which are typically used to gauge fracture toughness. To compare the results with those obtained using three-point bend tests, the value for the modulus and the fractures toughness are also determined by using the indentations methods (Vickers and nanoindentations). We computed other properties and compared them to known properties using the results of flexure and indentation. The testing of the microscales mechanical property is described in the study. The following analyses are applied to specimens made of other materials or made in different ways.

2. Experimental Techniques

As previously described [13, 15], bulks SAM2X5 sample were created using the spark of plasma sintering's (SPS). Gas atomization was used to create SAM2X5 powders, which were then ground in the Fritsch's P5 planetary and high energy balls mill. After milling, SAM2X5 powders particle are about 20μm in the size. These powders were subjected to sintering tests using the Sugimoto's SPS 1050 and SPS units (Sumitomo's Coal Mining's Co. Ltd., Japan), which produced discs with a thickness of around 2 mm using the 19 mm of inner diameter graphite dies and is lined with graphite paper. 9 g of powder, on average, were present in each sample. The applied load was 20 KN, and the sintering temperature was 600 °C. The samples were cylinder-shaped, with a diameter of 19 mm and a thickness of 2 mm. An immersion method was used to gauge the density of the SAM2X5 sample. The amorphous structure was evaluated using the X ray diffractions (XRD) pattern from the Rigaku Ultima IV systems utilizing CuK radiations and the scan rate of the one per second. For the evaluating the impacts of the mechanical grindings and the diamonds lapping on the sample's crystallization, the XRD of bulk of the samples were carried out as prepared and rough grounded (400 grit) with the diamonds lapped disc. On the thin foils sample that had been dimpling with ion-milled, TEM imaging's with the SAED were carried out utilizing the JEM 2100 F (JEOL) apparatus. For bend testing, the two bulks X ray amorphous such as SAM2X5 sample (Samples 1 & 2) was chosen. Our samples are given the SAM2X5 designation by our previous naming policy [13]. Because of their slow removal rate and the low heat production when used, surfaces lapping and the wire saw cuttings were used to reduce the effect of the heat production and deformations. The diamond paste was first used to lap the two samples until they were 1860 m thick and their surface was parallel within 1m over 20mm. To conduct experiments on modulus and fracture toughness, the sample was subsequently divided into the small specimen using the wire saw and Sic slurry. The bulk sample were divided into the six specimens for the flexural modulus of four specimens for fractures toughness, other samples were divided into the three specimens each for the flexural modulus with fractures toughness. The Flexural modulus specimen was rectangular in shape, 1860 mm by 500 mm cross sections in width and thickness, and 10 mm test gauge lengths. Although

specimens were approximately twice as small as the normal sizes' and have cross section of the 1mm and 1860 m (width & thickness, respectively), the gauge length of the 8 mm, and fractures toughness specimen are adhered to ASTM E399 prescribed ratios. Using a wire saw with the 50 mm diameter wires and the cuttings slurry of the 800 grit Sic powders (suspended in the oil) with the medium particles size of the 6.5 mm, fracture toughness specimens were notched. Using optical microscopy, the precise measurements of the ensuing notches revealed that there was 900 m in depth (about the half of the specimens thickness), 100 m in width, and has notched root radii of the 40m. To measure modulus and the fractures toughness of millimetre scale specimen, a specially designed and constructed small scales mechanical test apparatus was created. The device is comparable with testing of equipment used by the Eberl et al. [24] to evaluate thin films. The microbending machine with sample is shown in Fig. 1.

Fig. 1 Microbending machine, close-up of fracture toughness stage and sample

The stage's movement is controlled by the actuators, which are managed by MATLAB software. To track strain, cameras were employed for the digital images correlation (DIC) [24]. Due to an early fracture, the ASTM E399-specified fatigue cracks were not obtained. As a result, the reported toughness values are for notch toughness. To contrast the modulus and toughness information received from bending testing, indentation (Vickers and nanoindentation) was carried out. The samples were ground with SiC paper of 200, 400, 600, 800, & 1200 grits, then polishes with the suspensions of 1 mm diamond particles. The polished samples were subjected to Vickers indentations using the Leco LM100 indenters. Nine Vickers indentation was created for each sample using a 300 g load and a 10 s dwell duration. By Using the optical measurement of typical crack length originating from indents corner, indentations of toughness were estimated from the averages of nine Vicker indents of each sample. Anstis et al model's [4, 25], in which half penny of crack shape was assumed, and indentations toughness could be calculated based on it, and is one of most often used methods for the approximation of fracture toughness of BMGs.

$$K_c = \alpha \frac{P}{C_0^{3/2}} \sqrt{\frac{E}{H}} \tag{1}$$

where P is indentations load, H is hardness, E is modulus, c_0 is half fractures length; Kc is toughness estimated from the indentations; and α (0.016 ± 0.004) is calibrations constant with the (empirical constants). A Hysitron Triboindenter was utilized to create nanoindentations, which were then used to calculate the hardness and Young's modulus. For each of the two bulk samples, a total of 36 nanoindenters were created by using the Berkovich tips with a 200nm radius, the constant loading rates of the 1000 μN/s, and the maximum loads of 7500 μN. The maximum forces divided by area functions served as the basis for calculating hardness. Based on the area function and the stiffness of the unloading curve, reduced modulus as determined by nanoindentation was computed. The lowered modulus was then used to derive Young's modulus (under the assumption that v= 0.3). We used our three-point bending equipment to determine the flexural specimens' Young's modulus. 5 μm/s was the cross-head stage's movement rate. The movements of piezo actuators served as the basis for calculating displacement values. For each modulus test, a load-displacement curve was created by the subtracting compliance of machines, which was determined independently, from the data from the load cell. The following formula was used to determine Young's modulus for the supported prismatic beams with the rectangular cross-section based on the beam bending theory:

$$E = \frac{L^3 m}{4bd^3} \tag{2}$$

where the L is support's length, m is load-displacement curve's slope, b is the specimen's width, and d is its thickness. Using a 6061-T6 aluminium specimen that was cast as cast and had a shape identical to the SAM2X5 specimens, the apparatus and testing procedures were calibrated. For 6061-T6 Al, the Youngs modulus value obtained from our testing apparatus were within 3% of standard values of the 69 GPa [26]. it shows sample's top surfaces as well as how it was loaded for the measurements of fractures toughness. For these measurement, cross head stages were moved at the speed of 2μm/s. The displacement of the crack's mouths opening was measured using the DIC. By comparing loads cell data to DIC data, the load versus cracks mouth openings displacement curves were developed. Fracture toughness was calculated for each specimen using recorded peak loads by ASTM E399 guidelines.

3. Findings and Analysis

The SAM2X5-600 samples utilized in this work had a bulk density of 7.9 g/cm3, which is in good agreement with our earlier findings, which take into account of both theoretical values for SAM2X5 powders (7.75 g/cm3) and the structural relaxations which takes place throughout the consolidations processes [13, 15]. The same method of the processing was employed in [13] to create an amorphous alloy. Our earlier research supports the fully dense samples and illustrates microstructure of SAM2X5. The XRD profiles of the samples are shown in lower insets of the Fig. 2. The amorphous natures of SAM2X5 sample as seen in bright field TEM images is also depicted in Fig. 3

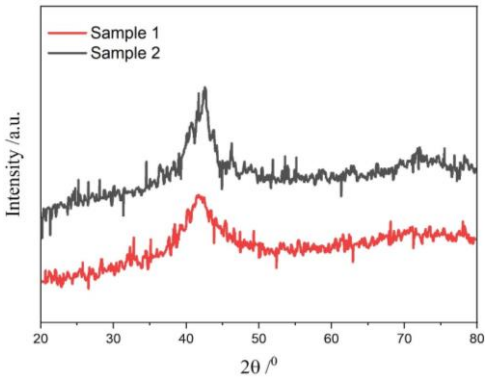

Fig. 2 The XRD plots of SAM2X5 BMGs indicating amorphous morphology

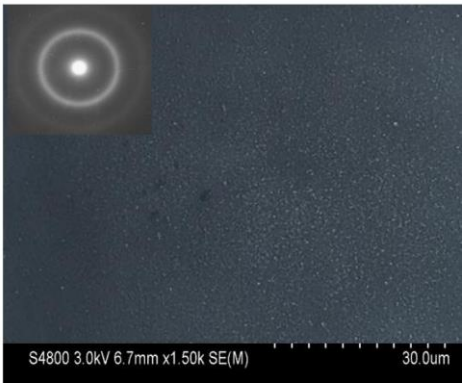

Fig. 3 TEM image, inset SAED pattern

The Diffusion ring with some of the diffraction's spots can be seen in the insets of SAED patterns of relevant regions. This show that the final product has mixtures of nanograins and amorphous structures and is not entirely amorphous. We assume that the final sample is primarily amorphous even though we do not statistically evaluate volumes percent of the amorphous vs nanograins. The BMG samples were made under various sintering settings (changing time and temperature). The optimal sintering conditions were found using XRD findings for broad diffraction peaks with few crystalline peaks, which are at the 600 °C. The insets of SAED patterns in Fig. 3 showed some crystallinity. But using SPS, this was the best the authors could come up with. Even though the presence of crystalline particles can have a negative impact on its toughness, and this is crucial for assessing the material's globally rather than the local toughness because estimates of the parts of life depends on global fractures toughness value. The measured fracture toughness values on bigger specimens, which were bent three times, account for "defect" like crystallinity that would be the inevitable in synthesis of the BMGs, and this guarantees that the fractures toughness measurements obtained through the three points bending may be applied to the life forecasts of the components fabricated from our BMGs. The Grindings and lapping's did not alter the XRD's profile, indicating that there was no devitrification caused by these specimen preparation techniques. It is plausible to assume that since wire saw cutting generates the less heat than the rough grindings, devitrification is also not a result of this operation. Youngs modulus value obtained by three-point bending have an average rate and the first standard deviation of the 227.3 ± 21.3 GPa for six of specimen made from the Sample 1 & 232.3 ± 22.2 GPa for the three-specimen made from Sample no 2. We use average numbers as reliable approximations of the 230 GPa, or Youngs modulus. Average and the standard deviation of the Youngs modulus value obtained from nanoindentations, in contrast, there are 276.5 GPa & 303.3 GPa, respectively. Result from nanoindentations is roughly 20–30% better than those from three-point bending. Standard deviations and average Vickers hardness values, respectively, were 11.16 ±0.21 GPa and 12.21± 0.21 GPa. Youngs modulus of the metallic glass can be calculated using Vickers hardness (E ≅ 20 Hv) [27]. The projected

Young's modulus, that are great agreements with the 230 GPa values discovered by our flexures testing, is between 220 GPa and 240 GPa based on the hardness values discovered by micro indentation. Alternately, the weighted modulus of the alloy elements can be used to approximate Youngs modulus [27]. This method yields Youngs modulus for the SAM2X5 of the 300 GPa, that is much in the line with our findings from nanoindentations. According to calculation, Vickers hardness is a good way to gauge Youngs modulus of bulk material, while the weighted Youngs modulus utilizing alloys components yields an accurate representation of the Youngs modulus measured by the nanoindentations. The average of hardness value obtained by the nanoindentations was greater than Vickers values at 18.0 GPa and 19.1 GPa, respectively. When utilizing the hardness relationship outlined above, hardness numbers don't replicate Youngs modulus result obtained via flexures. Fig. 4 shows the SAM2X5 nano indenter. Along the margins of the indent, the material has accumulated. On our SAM2X5 sample, Fig. 4 depicts material accumulation along the boundaries of a nano indenter. Youngs modulus and the hardness is measured by the nanoindentations can be overestimated by material accumulation. These effective contact areas of nano indenters is altered by significant flexibility, which causes the hardness to be overstated by up to 50% [28]. The assessment of the indent areas is challenging with nanoindentation due to pile-ups, and as a result, the hardness values obtained are not accurate. In light of this, hardness levels determined by the Vickers indentations with the higher force of 300g may be much more accurate. By Giving the direct correlation between Youngs modulus and the hardness and the nanoindentations measured Young's modulus is 20–30% higher, we estimate that the hardness is also 20–30% greater.

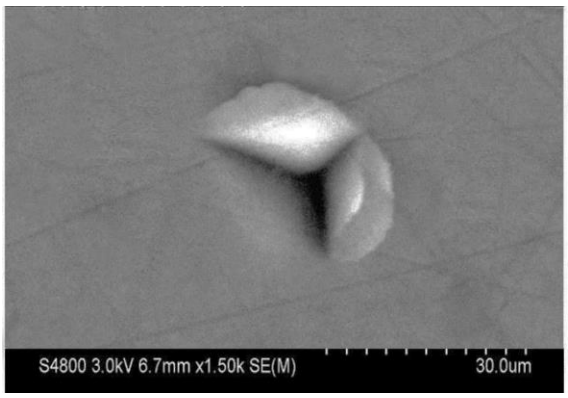

Fig. 4 Nanoindent of SAM2X5. Material pile-up can be observed along the edges of the indent

After adjusting for the 20–30% discrepancy, the hardness values for Samples 1 and 2 are 14–15 GPa and 15–16 GPa, respectively. The Young's moduli obtained by applying the $E \cong 20H$ relationships to the corrected hardness value range from about 280.0 GPa to 300.0 GPa and 290.0 GPa to 320.0 GPa, respectively. This Young's modulus is now more consistent with hardness result obtained by the nanoindentations (276.5 with 9.4 GPa and 303.3 with 9.1 GPa). The loads displacement curves for the flexural modulus test is

shown in Fig. 5. A sudden brittle failure is visible on all flexural modulus curves. None of the modulus test specimens showed any appreciable plastic deformation. Young's modulus and the glass transition temperature are both inversely correlated (Tg = 2.5E, where Tg is in the Celsius and the E is in GPa) [27]. The glass transitions temperature of the 575 °C was obtained by using ours observed Youngs modulus by the flexure or Vickers indentations (230 GPa) and the Tg = 2.5E relationships, which are very good agreements with previously report glass transitions temperature of the 580 °C for this type of material [29]. By using the direct nanoindentation results, this method would greatly overstate the glass transition temperature, which justifies the adoption of our correction. A typical load vs cracks mouth displacements curve for the fracture toughness tests utilizing three points bending's is shown in Fig. 5. The load against crack mouth displacement curves for all of the fractures toughness test in this study show no changes in the slope before failure, which is consistent with brittle failure at the peak stress. For Samples 1 and 2, the average fractures toughness value determined by three points bending are the 5.0 ±0.7 $MPam^{1/2}$ and 4.7 ±0.8 $MPam^{1/2}$, respectively.

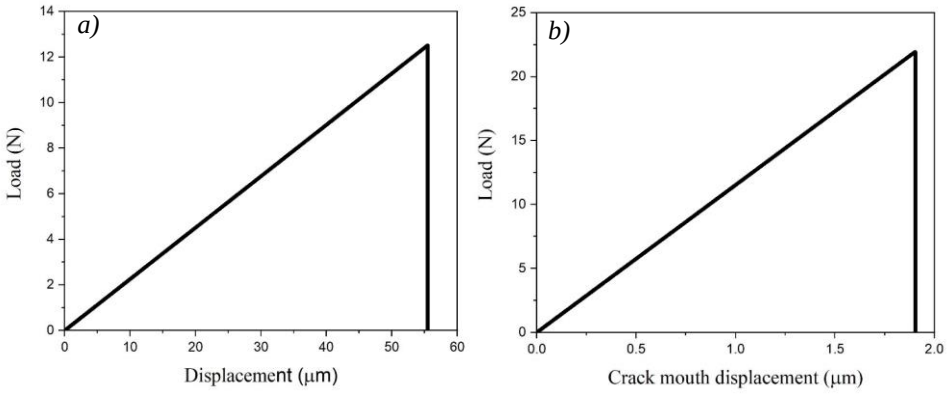

Fig. 5 (a)Flexural modulus and (b) fracture toughness load versus displacement curves for SAM2X5 samples tested by three-point bending.

The difference between the two samples is negligible. Therefore, we choose 4.9 MPa.m1/2 as the average values for the notch fracture toughness. Both bulk samples had average indentation (Vickers) toughness values of 2.5 ±0.1 MPa m1/2 and 2.2 ±0.1 MPa m1/2, respectively. The FeB-based BMGs (SAM2X5) have been demonstrated to be more brittle and stronger than FeC and the FeC(B)-based BMGs [30]. As anticipated, SAM2X5 (a FeB-based BMG) has exhibited Vickers indentation toughness values that are slight lower than the those of other FeC-based BMGs [16, 18]. The Quinn and Bradt [30] the point out that it is doubtful that Vickers toughness values are true or valid, except from by chance. We discover that these values are 50% less than those we obtain from ours three points bend test. There is a significant degree of inaccuracy in indentation toughness tests [32]. For instance, it can be challenging to get the required half-penny crack geometries, and the computation does not take the irregular and the secondary crack into account (cracks branching). The crack coming from the Vickers indents are depicted in Fig. 6. Half cracks length is optically determined as the separations between

indentation's centres and cracks' tips. The assumption made which calculates fractures toughness, is which where the crack that form corners of the indent which are straight with the same lengths. Vickers indents caused cracks to emerge in our SAM2X5 samples, and these irregular cracks added to the computed fracture toughness values' inaccuracies. Accurate measurement of the crack lengths is one of the flaws in the Vickers indentation toughness determination process. This was the primary impetus for the creation of the micromechanical tester, which more precisely measures toughness levels. This is a problem not only in this study but in other studies that use indentation to measure fracture toughness. Based on the research of Anstis et al. [25], indentation fracture toughness results are only reliable around ±40% of the time. The "calibration" constant (α) employed in the half crack length, it should be mentioned. Vickers indentation data of the fracture toughness of half a crack are shown in Fig. 6.

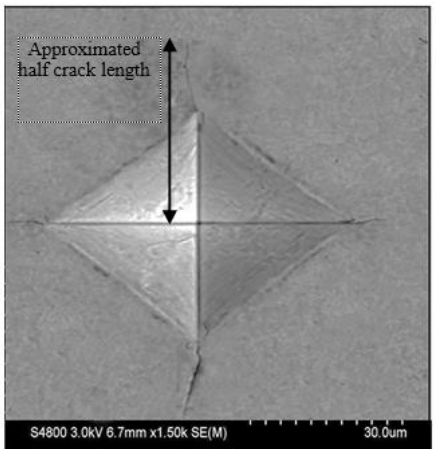

Fig. 6 Fracture toughness measurements of half crack length using Vickers indentation. Cracks emanating from corners of Vickers indents are seldom straight nor symmetric about the center.

Vickers indents' corner cracks are rarely symmetrical or straight around the centre. It is noted that the “calibration” constant (α) used is taken to be independent of material. In actuality, this value depends on the material and is chosen by comparing it to approved values discovered during bending experiments. Vickers indentation assessment of fracture toughness is therefore accurate when it is known, which was not the situation for the many BMGs, where the samples size precludes bending’s experiments. It has been demonstrated that accuracy of indentations findings derived using the common "calibrations" constant of α(0.016) deviates from typical ASTM KIC measurements of SiC samples by around 50% [31, 33]. Therefore, it has been demonstrated that mechanical property of Zr based BMGs are influenced by sample size. For the Zr-based BMG wire and foil less than the 1 mm in sizes, Conner et al. [34, 35] demonstrated a notable increase in the bends ductility. That is, as the sample size was decreased below the samples thickness of approximately 1mm, the plastic strains to the fractures in bending increased dramatically. According to ASTM, measurements of fracture toughness

acquired by the three points bending of specimen of at least 1mm in length were more equivalent to the measurements made during the large-scale testing, but measurements made by indenting are not indicative of bulk characteristics. upon the impact of the notched versus fatigues pre-cracked specimen on the fractures toughness measures of the Zr-based BMGs, varying results have been reported. According to reports, the fractures toughness value of the notched sample of different widths are higher (2x) than those of fatigue-pre-cracked samples [36, 37]. The discrepancies in failure mechanisms at the notched roots were one explanation for the disparity in toughness levels. Planar crack fronts were present in the fatigue pre-cracked samples in [35], whereas considerable crack bifurcations and shear bands were present in the notched samples. The authors proposed that the variations in observed toughness values could be explained by the energy absorptions from the shear bands and cracked bifurcations in the notched sample. However, additional studies [38] in the Zr based and the Ti-based BMGs have likewise found no discernible differences in the observed fractures toughness of the notched versus fatigues pre-cracked sample. Both the notched and the fatigue pre-cracked samples in those investigations displayed extremely high ductility, displaying pronounced shear banding for the both type of samples. The Energy absorptions and the thus assessed toughness level was comparable because the failures mechanisms for the both type of sample was the same. For the extremely brittle BMG like Fe based BMG, there hasn't yet been a study that compares the toughness value of the notched vs fatigues pre-cracked specimen (according to the ASTM E399). The SAM2X specimens that were notched were not fatigue pre-cracked by us. Although no shear banding or crack bifurcation was seen in any of the notch toughness specimens examined in this study, all of them showed planar crack fronts, suggesting failure processes comparable to those of the fatigue pre-cracked specimens on Zr-based BMGs reported in [36]. As a result, even though the current work's toughness specimens lack fatigue cracks, the way cracks spread suggest that the notched toughness value would be consistent with the toughness value for the SAM2X5 specimen that have fatigue cracks. Nishida et al. [39] examined the impact of the notched root radius of the fracture’s toughness of the fine-grained ceramics with the fracture’s toughness values comparable to the SAM2X. The Sintered Al2O3 sample with the grain sizes of the 1 μm was evaluated utilizing the notch with a range of the root radii (3 μm to 100 μm) using a method identical to ours. The researchers discovered that, below 10 m, values were stable, and fracture toughness declined with decreasing notch root radius. The difference between a root radius of 40 micrometres (as in the current study) and one of 10 micrometres (as in the study) decreased by around 25%, suggesting that the notched toughness values were measured are likely overstated. For more reliable fracture toughness measurements in future, a tiny (sharp) notched root radius (approaching fatigues pre-crack) was preferred. A figure that is 25% lower than what we recorded would result from assuming the sharper roots radius (i.e., less than the 10 μm), which would be simulating fatigue crack. There it appeared to be a lower limit to the relationship between fracture toughness and notch root radius. Result from the sintered Al2O3 systems indicates that the values measured below the 10μm were identical. According to the theory, fracture toughness values would be comparable as long as notched root radius which is small enough to create same crack "systems" as the fatigues pre-cracked instance. We made sure that the notched root radius was as small as possible because fatigue cracks on the specimens for fracture toughness could not be obtained. Our

SAM2X5 specimens show planar crack fronts without shear banding. We, therefore, think that the results of our three-point bending are fairly close to the results of specimens that had undergone fatigue cracking. Three-point bending fracture toughness values may be lower when using a much sharper notch, but we are unsure exactly how much less. However, by employing the three-points bending, we had removed several potential sources of the error in the Vickers indentations, including poorly defined as the crack length and the calibration values that could produce value that differs by either + or -40% of "real" values. We are aware that the notched root radius, which has made an effort to reduce as much as reasonable, maybe the primary cause of the error. Since SPS SAM2X5's absolute fracture toughness cannot currently be measured, we have believed that measuring fractures toughness using our method will result in the more accurate values. We have also provided estimates of the size of the errors and the potential directions of the real values. Therefore, it would be very advantageous to apply this method described in the paper for measuring fractures toughness to other brittle bulk metallic glasses.

Nanoindentation measurements were used to map the hardness and modulus in two dimensions to look at the impact of tungsten on the SAM2X5 matrix, as shown in Fig. 7 the typical loading curves for the two stages. To examine the mechanical characteristics of the SAM2X5 matrix phase, the hardness and modulus maps from a 10 x 10 or 15 x 15 nanoindentation array with a spacing of 4 μm were prepared. Nanoindentation has been utilized by many authors to examine BMGs [9,33–35,40]. For instance, a large soft zone and local core of a shear band have been studied using a mapping of nanoscale structural characteristics [2]. Recent researches have used the 3-D contour function to assess how heterogeneous structure affects the amorphous matrix phase.

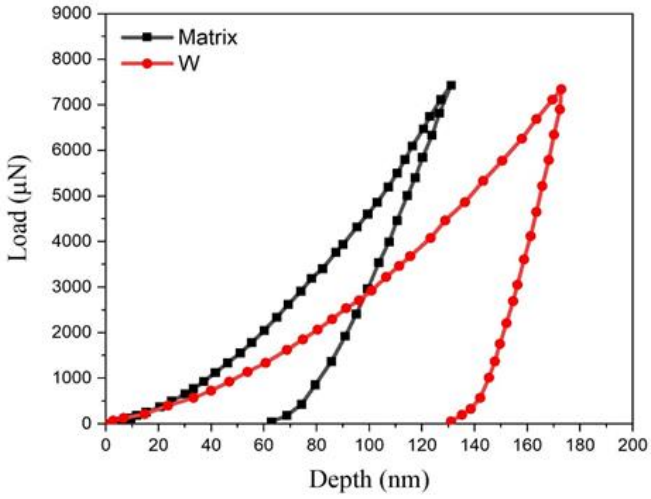

Fig. 7 Typical loading curves in the two phases

A Weibull curve of the SAM2X5-30%W composites' flexural strength or modulus of rupture (MOR) is shown in Fig. 8. From the Weibull plot, the characteristic strength, σo, and Weibull modulus, m, were calculated to be 165 and 8.7 MPa, respectively.

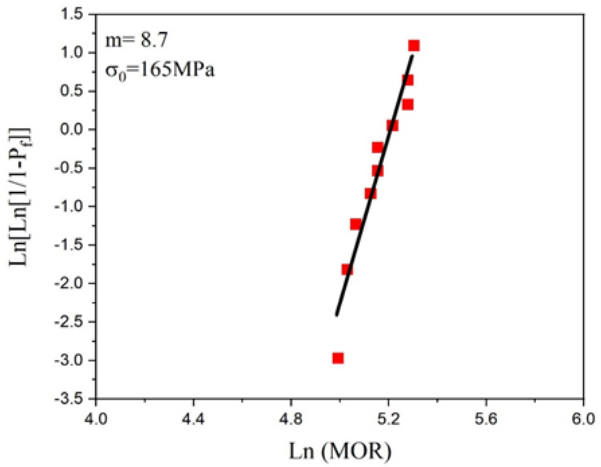

Fig. 8 Weibull plot for modulus of rupture (MOR) calculated for the SAM2X5/30%W composites.

4. CONCLUSION

For the Fe based bulk metallic glasses, the flexural modulus and the fractures (notch) toughness were calculated to be the 230 GPa and the 4.9 $MPam^{1/2}$, respectively. The Flexural modulus measurements were much lower and more accurate representations of bulk properties than those obtained using nanoindentation. The testing procedures and specimens for fracture toughness were as close to ASTM E399 requirements as possible. With all ratios as recommended, the specimen's size is roughly half of the recommendation's values. Three-point bending measurements of the notched toughness of the specimen without the fatigue cracks (4.9 $MPam^{1/2}$) with the relatively sharp notched root radii of (40 μm) are more accurate than Vickers indent measurements of fracture toughness (50 percent lower). The observed variations between three-point bending measurements and indentation measurements are anticipated. Due to the large specimen's size, specimens' geometries such as (rectangular versus the circular), and the specimen's preparation, bulk of the fracture's toughness and the modulus measurements of the BMGs utilizing our new testing techniques are much more precise than the value measured by indentations. The inclusions and flaws that are more likely to be present in our larger specimen size make the measured values for fracture toughness more indicative of the entire sample. There are a few sources of measurement of errors for the crack tips in rectangular specimen's geometries compared to cylindrical specimens because they have constant cross sections. Finally, specimens' preparations utilizing the wire saw cutting reduce the amount of the damage layer by minimizing plasticity and heat damage in comparison to other laboratories' usage of EDM.

Acknowledgments: *This work is supported by the National Key Research and Development Project (2020YFC1521900 & 2020YFC1521904), the National Nature Science Foundation (51902259), the 111 Program (B08040) of MOE of China. Here we also express appreciation for the Analytical & Testing Center of Northwestern Polytechnical University for SEM and XRD tests.*

REFERENCES

1. Tönnies, D., Samwer, K., Derlet, P. M., Volkert, C. A., Maaß, R., 2015, *Rate-dependent shear-band initiation in a metallic glass*, Appl. Phys. Lett., 106(17), 171907.
2. Suryanarayana, C., Inoue, A., 2013, *Iron-based bulk metallic glasses*, Int. Mater. Rev., 58(3), pp. 131-166.
3. Blink, J., Farmer, J., Choi, J., Saw, C., 2009, *Applications in the nuclear industry for thermal spray amorphous metal and ceramic coatings*, Metall. Mater. Trans. A, 40(6), pp. 1344–1354.
4. Phan, T. Q., Kelly, J.P., Kassner, M.E., Eliasson, V., Graeve, O.A., Hodge, A.M., 2016, *Bulk mechanical properties testing of metallic marginal glass formers*, J. Metall., 6508597.
5. Qiu, K.Q., Pang, J., Ren, Y.L., Zhang, H.B., Ma, C.L. Zhang, T., 2008, *Fe-based bulk metallic glasses with a larger supercooled liquid region and high ductility*, Mater. Sci. Eng. A, 4981–2), pp. 464-467.
6. Li, X., Kato, H., Yubuta, K., Makino, A., Inoue, A., 2011, *Improved plasticity of iron-based high-strength bulk metallic glasses by copper-induced nanocrystallization*, J. Non. Cryst. Solids, 357(15), pp. 3002-3005.
7. Guo, S. F., Liu, L., Li, N., Li, Y., 2010, *Fe-based bulk metallic glass matrix composite with large plasticity*, Scr. Mater., 62(6), pp. 329-332.
8. Hofmann, D. C., Suh, J.-Y., Wiest, A., Lind, M.-L., Demetriou, M. D., Johnson, W.L., 2008, *Development of tough, low-density titanium-based bulk metallic glass matrix composites with tensile ductility*, Proc. Natl. Acad. Sci., 105(51), pp. 20136-20140.
9. Schuh, C.A., Nieh, T.G., 2004, *A survey of instrumented indentation studies on metallic glasses*, J. Mater. Res., 19(1), pp. 46-57.
10. Zhang, C., Liu, L., Chan, K.C., Chen, Q., Tang, C.Y., 2012, *Wear behavior of HVOF-sprayed Fe-based amorphous coatings*, Intermetallics, 29, pp. 80–85.
11. Wang, A.P., Chang, X.C., Hou, W.L., Wang, J.Q., 2007, *Preparation and corrosion behaviour of amorphous Ni-based alloy coatings*, Mater. Sci. Eng. A, 449, pp. 277-280.
12. Turek, P., 2021, *Evaluation of the auto surfacing methods to create a surface body of the mandible model*, Reports in Mechanical Engineering, 3(1), pp. 46-54.
13. Komaki, M., Mimura, T., Kurahasi, R.., Kouzaki, M., Yamasaki, T., 2011, *High chromium Fe-Cr-Mo-PC amorphous coating films produced by thermal spraying technique*, Mater. Trans., 52(3), pp. 474-480.
14. Graeve, O.A., Kanakala, R., Kaufman, L., Sinha, K., Wang, E., Pearson, B., Gabriel, R-G, Farmer J.C., 2008, *Spark plasma sintering of Fe-based structural amorphous metals (SAM) with Y2O3 nanoparticle additions*, Mater. Lett., 62(17–18), pp. 2988-2991.
15. Graeve, O.A., Saterlie, M.S., Kanakala, R., De La Torre, S.D., Farmer, J.C., 2013, *The kinetics of devitrification of amorphous alloys: the time–temperature–crystallinity diagram describing the spark plasma sintering of Fe-based metallic glasses*, Scr. Mater., 69(2), pp. 143-148.
16. Kelly, J.P., Fuller, S.M., Seo, K., Novitskaya, E., Eliasson, V., Hodge, A.M., Graeve, O.A., 2016, *Designing in situ and ex situ bulk metallic glass composites via spark plasma sintering in the super cooled liquid state*, Mater. Des., 93, pp. 26-38.
17. Keryvin, V., Hoang, V.H., Shen, J., 2009, *Hardness, toughness, brittleness and cracking systems in an iron-based bulk metallic glass by indentation*, Intermetallics, 17(4), pp. 211-217.
18. Keryvin, V., Vu, X.D., Hoang, V.H., Shen, J., 2010, *On the deformation morphology of bulk metallic glasses underneath a Vickers indentation*, J. Alloys Compd., 504, pp. S41-S44.
19. Liu, C.Y., Zhang, Y.X., Yuan, G., Zhang, C.Y., Misra, R.D.K., 2022, *Microstructure and properties of ultra-thick Fe-based metallic glass by twin-roll strip casting versus a traditional process*, Mater. Res. Bull., 153, 111878.
20. Shamimi Nouri, A., Gu, X.J., Poon, S.J., Shiflet, G.J., Lewandowski, J.J., 2008, *Chemistry (intrinsic) and inclusion (extrinsic) effects on the toughness and Weibull modulus of Fe-based bulk metallic glasses*, Philos. Mag. Lett., 88(11), pp. 853-861.

21. Chen, W., Ketkaew, J., Liu, Z., Mota, R., Bien, K.O., sene da silva, C., Schroers, J., 2015, *Does the fracture toughness of bulk metallic glasses scatter?*, Scr. Mater., 107, pp. 1-4.
22. Kawashima, A., Kurishita, H., Kimura, H., Zhang, T., Inoue, A., 2005, *Fracture toughness of Zr55Al10Ni5Cu30 bulk metallic glass by 3-point bend testing*, Mater. Trans., 46(7), pp. 1725-1732.
23. Narayan, R.L., Tandaiya, P., Garrett, G.R., Demetriou, M.D., Ramamurty, U., 2015, *On the variability in fracture toughness of 'ductile' bulk metallic glasses*, Scr. Mater, 102, pp. 75-78.
24. Eberl, C., Gianola, D. S., Hemker, K.J., 2010, *Mechanical characterization of coatings using microbeam bending and digital image correlation techniques*, Exp. Mech., 50(1), pp. 85-97.
25. Ast, J., Ghidelli, M., Durst, K., Göken, M., Sebastiani, M., Korsunsky, A.M., 2019, *A review of experimental approaches to fracture toughness evaluation at the micro-scale*, Mater. Des., 173, 107762.
26. Das, M., Mishra, D., Mahapatra, T. R., 2019, *Machinability of metal matrix composites*, Materials Today: Proceedings, 18, 5373-5381.
27. Wang, W.H., 2012, *The elastic properties, elastic models and elastic perspectives of metallic glasses*, Prog. Mater. Sci., 57(3), pp. 487-656.
28. Sudharshan Phani, P., Oliver, W.C., Pharr, G.M., 2021, *Measurement of hardness and elastic modulus by load and depth sensing indentation: Improvements to the technique based on continuous stiffness measurement*, J. Mater. Res., 36(11), pp. 2137-2153.
29. Farmer, J.C., Haslam, J., Day, S., Lian, T., Saw, C., Hailey, P., Lavernia, E.J., Ajdelsztajn, L., Branagan, D.J., Buffa, E.J., Aprigliano, L., 2007, *Corrosion resistance of thermally sprayed high-boron iron-based amorphous-metal coatings: Fe49.7Cr17.7Mn1.9Mo7.4W1.6B15.2C3.8Si2.4*, J. Mater. Res., 22(8), pp. 2297-2311.
30. Guo, S. F., Qiu, J. L., Yu, P., Xie, S. H., Chen, W., 2014, *Fe-based bulk metallic glasses: brittle or ductile?*, Appl. Phys. Lett., 105(16), 161901.
31. Quinn, G.D., Bradt, R.C., 2007, *On the Vickers indentation fracture toughness test*, J. Am. Ceram. Soc., 90(3), pp. 673–680.
32. Kruzic, J.J., Kim, D.K., Koester, K.J., Ritchie, R.O., 2009, *Indentation techniques for evaluating the fracture toughness of biomaterials and hard tissues*, J. Mech. Behav. Biomed. Mater., 2(4), pp. 384-395.
33. Yang, X., Liu, X., Huang, Z., Yao, X., Liu, G., 2013, *Vickers indentation crack analysis of solid-phase-sintered silicon carbide ceramics*, Ceram. Int., 39(1), pp. 841-845.
34. Conner, R.D., Li, Y., Nix, W.D., Johnson, W.L., 2004, *Shear band spacing under bending of Zr-based metallic glass plates*, Acta Mater., 52(8), pp. 2429–2434.
35. Conner, R.D., Johnson, W.L., Paton, N.E., Nix, W.D., 2003, *Shear bands and cracking of metallic glass plates in bending*, J. Appl. Phys., 94(2), pp. 904–911.
36. Lewandowski, J.J., Thurston, A.K., Lowhaphandu, P., 2002, *Fracture toughness of amorphous metals and composites*, MRS Online Proc. Libr., 754, 93.
37. Hashemi, K. S. H., 2021, *Nonlinear vibration response of piezoelectric nanosensor: influences of surface/interface effects*, Facta Universitatis-Series Mechanical Engineering, doi: 10.22190/FUME210612064K
38. Gu, X.J., Poon, S.J., Shiflet, G.J., Lewandowski, J.J., 2010, *Compressive plasticity and toughness of a Ti-based bulk metallic glass*, Acta Mater., 58(5), pp. 1708–1720.
39. Singh, D., Rao, P. V. A., 2007, *A surface roughness prediction model for hard turning process*, Int. J., Adv, Manuf, Technol., 32, pp. 1115-1124.
40. Li, J., Tang, X., 2023, *Research on Anti-Wear Properties of Nano-Lubricated High-Speed Rolling Bearings under Various Working Conditions*, Tehnički Vjesnik, 30(1), pp. 61-67.